Rapid Communications

Stochastic resonance via parametric adaptation: Experiments and numerics

Ishant Tiwari, J. M. Cruz,* and P. Parmananda
Department of Physics, Indian Institute of Technology, Bombay, Powai, Mumbai–400 076, India

M. Rivera
Centro de Investigación en Ciencias-(IICBA), UAEM, Avenida Universidad 1001, 62209 Cuernavaca, Morelos, Mexico

(Received 23 August 2019; published 6 December 2019)

In contrast with the conventionally observed mechanism of stochastic resonance (SR) wherein the level of additive noise is systematically varied with a fixed set-point parameter, in this work we report the emergence of the SR phenomena in an electrochemical system maintaining the same level of noise and varying the parametric distance from a homoclinic bifurcation inherent to the system. The experimental system involves the corrosion of a metal disk in an acidic medium under potentiostatic conditions. The applied potential is used as a control parameter and the anodic current generated during the electrodissolution of the metal is the accessible system variable. In the presence of noise, it was observed that the system was able to enhance its output's fidelity with a weak subthreshold input signal when the set point was kept at an optimal parametric distance from the bifurcation. Numerical simulations were performed on a model for this system to corroborate the experimental observations. This type of SR may be critical in scenarios where a biological entity has control only on its sensory parameters and not on the environmental noise amplitude.

DOI: 10.1103/PhysRevE.100.060202

Detection of weak signals in a noisy environment is an essential requirement for natural systems that are devoid of a conventional signal amplifying apparatus. One phenomenon that accomplishes this process is the mechanism of stochastic resonance (SR). The SR emerges from the interaction between the system's nonlinearity and internal or external stochasticity, resulting in the amplification of an otherwise undetectable weak signal. Benzi *et al.* reported this phenomenon in 1981 [1,2] to explain the periodicity of the Earth's glaciation cycles. These results were followed by the work of Nicolis and Nicolis later in the same year [3]. In these landmark articles, SR was reported in systems showing bistable behavior. The separatrix dividing the basins of attraction of the two fixed points acts as a threshold for the noise amplitude. The presence of such a threshold is critical in observing SR. It has now been reported in a diverse set of theoretical [4–9] and experimental [10–16] systems which create this threshold via different mechanisms, such as Hopf bifurcation [4,9,13] and homoclinic bifurcation [14,15,17,18]. SR is further categorized into periodic SR [1–3,13] and aperiodic SR [14,19] depending on the periodicity or aperiodicity of the input signal. In the absence of such an input signal, a relative enhancement in the coherence of the system's output at an optimal amplitude (level) of noise is called coherence resonance [18,20–22]. A detailed review over the topic of stochastic resonance and related phenomena can be found in a review written by Gammaitoni *et al.* [23].

Conventionally, SR refers to the optimization of input-output fidelity by varying the amplitude of the noise present in the system. This method of varying noise amplitude is of interest in cases where direct control over the noise strength is present. However, this direct control mechanism is hard to envisage in a biological agent for signal detection in its environment. Even when noise may be abundant in its environment, the individual may have little or no control over the noise amplitude to improve a signal's detection. In such a scenario, the agent might still be able to enhance the signal detection efficacy by optimizing its sensory parameters. A numerical demonstration of this mechanism was performed by Anishchenko *et al.* in 1993 [24] on the Chua's oscillator. Over the years, there have been further numerical studies in this direction, for excitable neuronal models [25,26] and bistable systems [9,27–29].

In the present work, we *experimentally* demonstrate the phenomenon of stochastic resonance by controlling a system parameter while keeping the level of noise in the system invariant. For this purpose, an electrochemical system involving the corrosion of iron in the presence of sulfuric acid and copper sulfate is used. It is observed that the system response has enhanced fidelity with a weak input signal (periodic or aperiodic) at an optimal parametric distance from a homoclinic bifurcation, while the noise amplitude (level) is maintained at a constant value. This observation is verified by calculating the cross-correlation coefficient between the signal and the system response at various set-point parameter values. The resulting curve is unimodal in nature with a maximum cross-correlation being achieved at an intermediate (optimal) value of the parametric distance. Numerical simulations have been performed in a model [30] developed for the experimental system to corroborate our results.

*Present address: Facultad de Ciencias en Física y Matemáticas, Universidad Autónoma de Chiapas, Tuxtla Gutiérrez, Chiapas 29050, Mexico.

 ©2019 American Physical Society

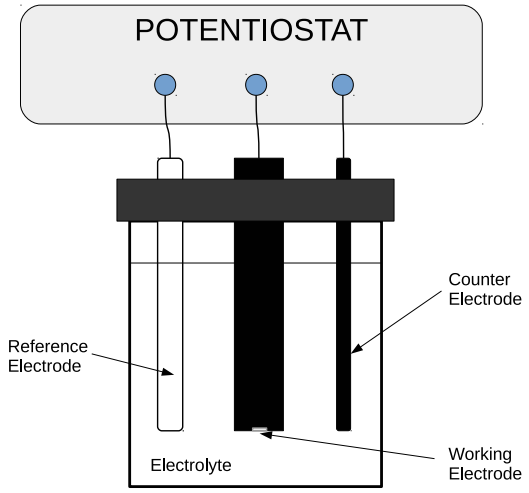

FIG. 1. A schematic of the experimental setup used to study the electrodissolution of an iron disk anode (working electrode) in an acidic media (electrolyte). Copper sheet and saturated calomel electrode are the cathode (counterelectrode) and the reference electrode, respectively. The applied potential is controlled with a potentiostat and a USB DAC control card (not shown).

The subsequent text is organized in the following order. First, the experimental setup and protocol are detailed, after which the experimental results involving periodic and aperiodic stochastic resonance are presented. Subsequently, the electrochemical model is explained and the numerical simulation analyses are shown. Finally, a brief summary and discussion of the obtained results are given.

The experimental setup consisted of a three-electrode electrochemical cell used to study the electrodissolution of iron in an acidic media. The anode (working electrode) was an iron disk with a diameter of 6.3 mm (Able Target iron rod, 99.9% purity) shrouded in epoxy. The circular cross-sectional surface was pretreated by polishing it with sandpapers of monotonically finer grits (grit sizes 280, 400, 600, and 1500) to create a smooth circular surface which gets exposed to the electrolyte. The cathode (counterelectrode) was a copper sheet (12 mm $\times$ 50 mm, 0.3 mm thickness) immersed in the electrolyte. The third electrode was a saturated calomel electrode which is used as a reference electrode. The electrolyte in which all three electrodes were immersed consisted of a mixture of 1.0 M sulfuric acid (Baker ACS, 97.9%) and 0.4 M copper sulfate pentahydrate (Baker ACS, 99.4%) solution. The electrolyte volume was maintained at 300 ml in all the experiments. The ambient temperature during the experiments was maintained at 298 K. A schematic of this setup is given in Fig. 1. Anodic potential with respect to the reference electrode was controlled with a Bi-potentiostat (Pine Instrument Co., AFRDE5). The applied potential V consisted of two types of signals: A constant value V_0 referred to as the set point of the system and a time-varying signal superimposed over it. The time-varying signal consisted of a weak (subthreshold) periodic or aperiodic rectangular pulse train $S(t)$ and a uniform white-noise signal $\eta(t)$ with zero mean and amplitude D. These time-varying signals were generated in a computer and supplied to the potentiostat using a control card (MCC-USB 3101) at a sampling rate of 100 Hz. The anodic current (I) was simultaneously recorded with a data acquisition card (MCC-USB 1608FS) at a sampling rate of 1 kHz. These experiments were performed at a fixed amplitude of external noise D while the set point V_0 was changed for each experimental run. The electrodes were polished and cleaned before each experiment to ensure quasi-identical initial conditions.

The autonomous dynamics, along with the bifurcations present in the system, have been reported previously in the work of Santos *et al.* [31]. The anodic potential is the system control parameter by the variation of which various dynamical regimes of the anodic current can be realized. A range of the potential values leads to period-1, limit cycle oscillations in the anodic current. This interval of potential lies within the parameter domain where the dynamical system exhibits fixed-point behavior. Within the oscillatory regime, the system exhibits relaxation oscillations with the period of oscillations increasing as one increases the anode potential V_0 [31]. This increment of period as a function of system parameter is indicative of the presence of a homoclinic bifurcation. It was previously demonstrated that the time period of these oscillations increases exponentially as a function of increasing anode potential V_0, until the cessation of oscillations is observed at V_{hc} [31]. At potentials higher than V_{hc}, the anodic current exhibits a fixed-point behavior. It is to be noted that although the exact locations of these bifurcations may vary from one experimental run to the other ($=305 \pm 2$ mV), the qualitative bifurcations are robust across all trials. In the present experiments, the system is kept at the fixed-point regime ($V > V_{hc}$). The anode voltage is $V(t) = V_0 + S(t) + D\eta(t)$, where V_0 is the set point of the system. $S(t)$ and $\eta(t)$ are the subthreshold signal (periodic or aperiodic) and external noise with amplitude D, respectively. The amplitude of noise D was kept constant for all experiments while the set point V_0 was varied to observe periodic or aperiodic stochastic resonance. For every set point, it was ensured that the subthreshold signal $S(t)$, by itself, was not sufficient to make the system cross the homoclinic bifurcation point V_{hc} [$V_0 + S(t) > V_{hc}$]. Hence, the bifurcation point V_{hc} was determined prior to the experiment in order to estimate the signal pulse amplitude $S(t)$ and the minimum value of the set point V_0 that is allowed.

For the case of periodic stochastic resonance (PSR), the signal $S(t)$ was taken to be a periodic train of rectangular pulses of amplitude -100 mV. The external noise amplitude D was kept fixed at 185 mV while the set point V_0 is systematically varied to observe PSR. The homoclinic bifurcation was located at $V_{hc} \approx 305$ mV. The pulse repetition interval (period) was 17 s with a pulse duration of 2 s. Different combinations of external noise amplitudes and interpulse intervals had been also explored in order to test the robustness of our experimental findings, showing similar results (not shown). In Fig. 2 (left), the top time series in red corresponds to a section of the subthreshold periodic signal $S(t)$. The panels (a)–(c) correspond to the system response (anodic current) at a low, optimal, and high set-point (V_0) value, respectively. Here, the set point is a measure of the parametric distance from the bifurcation V_{hc}. It is evident that there is maximal information transfer from the input signal to the system response at the optimal set-point value [Fig. 2, panel (b)]. At low values of the set point [Fig. 2, panel (a)],

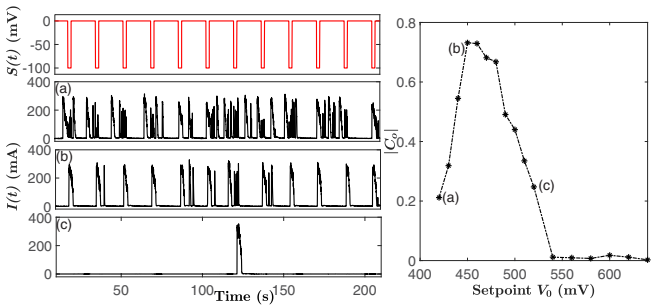

FIG. 2. Time series of the periodic input subthreshold signal (top left panel). System response (anodic current) to the input signal at low (a), optimal (b), and high (c) values of the set point V_0. The system response fidelity to the input signal is the best at the optimal set-point value. Cross-correlation coefficient ($|C_o|$) between the input and the output is plotted as a function of the set point V_0 in the right panel (dotted line). The curve shows a unimodal variation as a function of the set point with a maximum at $V_0 = 450$ mV, a characteristic observation of stochastic resonance. The marked points (a)–(c) on this curve correspond to the anodic current time series shown in the lower three panels on the left. The amplitude of noise was kept fixed at $D = 185$ mV while the input pulse amplitude was -100 mV. The time period between the pulses was 17 s with a pulse duration of 2 s.

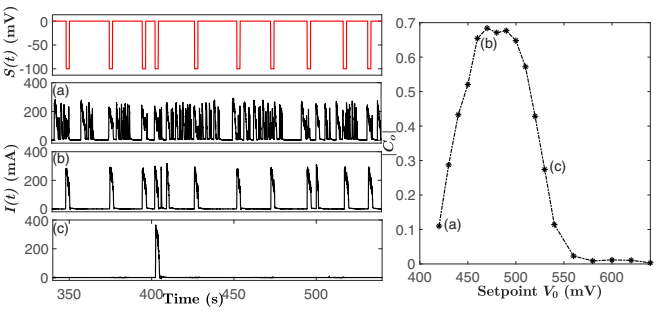

FIG. 3. Time series of the aperiodic input subthreshold signal (top left panel). System response (anodic current) to the input signal at low (a), optimal (b), and high (c) values of the set point V_0. The system response correlation to the input signal is the best at the optimal set-point value. Cross-correlation coefficient ($|C_o|$) between the input and the output is plotted as a function of the set point V_0 in the right panel (dotted line). The curve shows a unimodal variation as a function of the set point with a maximum at $V_0 = 470$ mV, indicating the occurrence of stochastic resonance. The marked points (a)–(c) on this curve correspond to the anodic current time series shown in the lower three panels on the left. The amplitude of noise was kept fixed at $D = 185$ mV while the input pulse amplitude was -100 mV. The time period between the pulses was uniformly distributed between 5 and 25 s with a pulse duration of 2 s.

the perturbed system responds even when the instantaneous value of $S(t) = 0$ due to the dominance of noise, leading to a decrease in the overall input-output correlation. In contrast, the system becomes insensitive to the subthreshold signal at higher values of the set point [Fig. 2, panel (c)]. This visual observation is verified by calculating the modulus of the cross-correlation coefficient ($|C_o|$) between the input subthreshold signal and the system response (anodic current) in Fig. 2 (right). The cross-correlation coefficient was calculated using the following formula applicable in the case of real signals using the MATLAB programming software:

$$|C_o| = \max[|\rho(\tau)|], \qquad 0 \leqslant \tau \leqslant 0.5 \text{ s},$$
$$\rho(\tau) = \frac{E\{[I(t) - \mu_I][S(t+\tau) - \mu_S]\}}{\sigma_I \times \sigma_S},$$

where $I(t)$ and $S(t)$ denote the anodic current and the input subthreshold signal, respectively. The function $E[\cdots]$ denotes the expectation value and σ and μ are the standard deviation and the mean of the respective quantities. The cross-correlation coefficient plotted as a function of the set point shows a characteristic unimodal shape with a clear maximum at $V_0 = 450$ mV. This observation is an indicator of the phenomenon of PSR.

To observe aperiodic stochastic resonance (ASR), the signal $S(t)$ was taken to be an aperiodic train of rectangular pulses of amplitude -100 mV while the noise amplitude D was kept fixed at 185 mV. The homoclinic bifurcation was found to be at $V_{hc} \approx 305$ mV. In this scenario, the input signal $S(t)$ was an aperiodic train of rectangular pulses with inter-pulse time intervals distributed uniformly randomly between 5 and 25 s with a mean value of 15 s. The pulse width was 2 s as kept for the case of PSR. In Fig. 3 (left), it can be observed that there is an optimal value of the set point V_0 at which there is maximal information transfer from the subthreshold signal to the system response (anodic current). This observation is corroborated by the presence of the characteristic unimodal shape of the $|C_o|$ versus V_0 curve [Fig. 3 (right)] with a maximum at $V_0 = 470$ mV. Therefore, it was demonstrated that the system response gets augmented fidelity with the input subthreshold signal at an optimal value of the system bifurcation parameter V_0 when the external noise amplitude D is kept constant.

To corroborate the experimental findings, a two-dimensional numerical model of the dynamics of an electrochemical cell under potentiostatic conditions was simulated [30]. This model captures the essential features of the experimental electrochemical cell studied in this work. The system equations are as follows:

$$\epsilon \dot{u} = \frac{v - u}{R} - f(u, c); \quad \dot{c} = \frac{u - v}{R} + (1 - c) + \alpha f(u, c),$$

where $f(u, c) = c(a_1 u + a_2 u^2 + a_3 u^3)$.

The variables $u(t)$ and $c(t)$ denote the electrode potential and the surface concentration of the electroactive species, respectively. The parameters ϵ, R, and v correspond to the double-layer capacitance, the Ohmic resistance, and the applied potential, respectively. The first equation corresponds to the conservation of charge, where the left-hand side corresponds to the current flowing through the double-layer capacitance. The first right-hand-side term refers to the total current flowing in the system and the second term corresponds to the Faradaic current due to the electrochemical reaction. The second equation gives us the mass balance where the first right-hand-side term is for diffusion and the second one is for the migration due to potential gradients. Further details along with corresponding bifurcations can be found in [30].

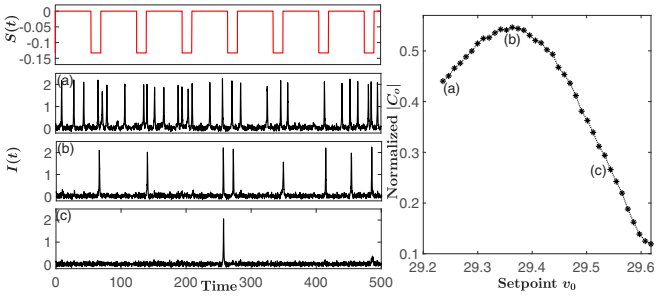

FIG. 4. Numerical simulations: Time series of the periodic input subthreshold signal (top left panel). System response (I) to the input signal at low (a), optimal (b), and high (c) values of the set point v_0. The system response correlation with the input signal is the best at the optimal set-point value. Normalized cross-correlation coefficient ($|C_o|$) between the input and the output is plotted as a function of the set point v_0 in the right panel (dotted line). The curve shows a unimodal variation as a function of the set point with a maximum at $v_0 = 29.36$, indicating the occurrence of stochastic resonance. Cross-correlation coefficient is normalized by the value of $|C_o|$ obtained for a superthreshold input signal and zero noise in the system. The $|C_o|$ curve (right panel) is an average curve after ten repetitions. The marked points (a)–(c) on the normalized $|C_o|$ curve correspond to the current time series I shown in the lower three panels on the left. The amplitude of noise was kept fixed at $D = 1.6$ while the input pulse amplitude was -0.133. The time period (dimensionless units) between the pulses was 70 with a pulse duration of 15.

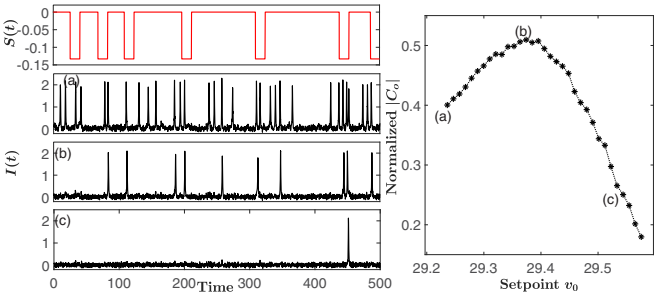

FIG. 5. Numerical simulations: Time series of the aperiodic input subthreshold signal (top left panel). System response (I) to the input signal at low (a), optimal (b), and high (c) values of the set point v_0. The system response correlation with the input signal is the best at the optimal set-point value. Normalized cross-correlation coefficient ($|C_o|$) between the input and the output is plotted as a function of the set point v_0 in the right panel (dotted line). The curve shows a unimodal variation as a function of the set point with a maximum at $v_0 = 29.37$, indicating the occurrence of stochastic resonance. Cross-correlation coefficient is normalized by the value of $|C_o|$ obtained for a superthreshold input signal and zero noise in the system. The $|C_o|$ curve (right panel) is an average curve after ten repetitions. The marked points (a)–(c) on the normalized $|C_o|$ curve correspond to the current time series I shown in the lower three panels on the left. The amplitude of noise was kept fixed at $D = 1.6$ while the input pulse amplitude was -0.133. The time period (dimensionless units) between the pulses was uniformly randomly distributed between 20 and 120 with a pulse duration of 15.

In this case, v is the bifurcation parameter of the system, and the anodic current I defined as $\frac{(v-u)}{R}$ is the observable. The model shows qualitatively similar dynamics to the experimental system at the parameter values $\epsilon = 0.03$, $\alpha = 0.1$, $R = 10$, $a_1 = 1.125$, $a_2 = -0.075$, and $a_3 = 0.001\,25$. A variety of dynamics can be provoked at different values of the bifurcation parameter v [30]. A limit cycle behavior is exhibited for $28.097 \leqslant v \leqslant 29.235$, beyond which the system exhibits stable fixed-point behavior. Noise and the input subthreshold signal were superimposed on the applied potential v in a similar fashion as the experiments, $v = v_0 + S(t) + D\eta(t)$. Here $S(t)$ and $\eta(t)$ represent the weak subthreshold signal (periodic or aperiodic) and uniform white noise with zero mean, respectively. The parameter v_0 can be considered as an analog of the system set point in the experiments. The parameters were chosen such that $v_0 + S(t)$ did not cross the bifurcation at $v = 29.235$. The system was simulated using the fourth-order Runge-Kutta method of solving ordinary differential equations in the presence of additive noise.

In these simulations the amplitude of noise D was kept fixed to 1.6 and the periodic (or aperiodic) signal amplitude was kept fixed to -0.133. To observe PSR (or ASR), the value of v_0 was varied while other system parameters remained constant.

As was done in the experiments, the observation of SR was quantitatively verified by calculating the cross-correlation coefficient ($|C_o|$) between the system response $I(t)$ and the input subthreshold signal $S(t)$. The value of $|C_o|$ was normalized with respect to the maximum achievable value of $|C_o|$ for a given signal and system parameters. This maximum achievable value was calculated by measuring the cross-correlation between the system response $I(t)$ and a *superthreshold signal* $S(t)$ in the absence of noise. A superthreshold signal is a signal whose amplitude is large enough to cause the output to spike whenever there is an input pulse without the presence of noise. Under these conditions, the system would respond to each pulse of the signal $S(t)$, hence it would yield the maximum achievable value of $|C_o|$. As seen in Figs. 4 and 5, we observe an augmented signal response with respect to the input subthreshold signal (periodic in Fig. 4 and aperiodic in Fig. 5) at an optimal value of the system set point v_0. A characteristic unimodal shape in the normalized $|C_o|$ versus set point v_0 curve is also observed in both the cases (right panel, Figs. 4 and 5). Therefore, numerical simulations of a simplified electrochemical model of an electrode operating under potentiostatic conditions yield results which are similar to our experimental observation of SR induced by varying a system set-point parameter.

In this work, we demonstrated the emergence of SR in a system where external additive noise amplitude remains fixed. This was done by varying a system parameter which controlled the system's parametric distance from a bifurcation. This type of signal detection can find its use in biological systems where an agent has to detect a weak signal in a noisy environment. Having little or no control on the environmental noise amplitude, augmenting its signal detection efficiency by adjusting its sensory parameters may be advantageous for a biological agent. This type of signal detection may also be relevant to systems with internal noise, such as ensembles of neurons. Internal noise sources are ubiquitous and usually out of the system's control. Hence, such systems may be good potential systems for further experiments in set-point parameter controlled stochastic resonance. In the context of

electrochemical systems, pitting corrosion on different substrates is regarded as a stochastic process. Considering this stochastic process as a source of internal noise, one can search for stochastic resonance phenomena similar to the present work by varying a system parameter while keeping the level of internal noise constant.

We would like to thank DST, India for financial support (Project No. EMR/2016/000275). I.T. gratefully acknowledges financial support from CSIR, India. J.M.C. acknowledges CONACYT (Repatriación 2019-1). The authors are thankful to the Non-Linear Dynamics Lab group in IIT-Bombay for their valuable suggestions.

[1] R. Benzi, A. Sutera, and A. Vulpiani, J. Phys. A: Math. Gen. **14**, L453 (1981).
[2] R. Benzi, G. Parisi, A. Sutera, and A. Vulpiani, Tellus **34**, 10 (1982).
[3] C. Nicolis and G. Nicolis, Tellus **33**, 225 (1981).
[4] D. Nozaki and Y. Yamamoto, Phys. Lett. A **243**, 281 (1998).
[5] R. F. Fox and Y. N. Lu, Phys. Rev. E **48**, 3390 (1993).
[6] G. Schmid, I. Goychuk, and P. Hänggi, Europhys. Lett. **56**, 22 (2001).
[7] J. M. Cruz, P. Parmananda, and T. Buhse, J. Phys. Chem. A **112**, 1673 (2008).
[8] S. Sinha, J. Cruz, T. Buhse, and P. Parmananda, Europhys. Lett. **86**, 60003 (2009).
[9] I. Tiwari, D. Dave, R. Phogat, N. Khera, and P. Parmananda, Chaos **27**, 103112 (2017).
[10] A. Simon and A. Libchaber, Phys. Rev. Lett. **68**, 3375 (1992).
[11] S. Fauve and F. Heslot, Phys. Lett. A **97**, 5 (1983).
[12] D. F. Russell, L. A. Wilkens, and F. Moss, Nature (London) **402**, 291 (1999).
[13] K. Wiesenfeld, D. Pierson, E. Pantazelou, C. Dames, and F. Moss, Phys. Rev. Lett. **72**, 2125 (1994).
[14] P. Parmananda, Gerardo J. Escalera Santos, M. Rivera, and K. Showalter, Phys. Rev. E **71**, 031110 (2005).
[15] I. Tiwari, R. Phogat, P. Parmananda, J. L. Ocampo-Espindola, and M. Rivera, Phys. Rev. E **94**, 022210 (2016).
[16] T. Roy, V. Agarwal, B. Singh, and P. Parmananda, Appl. Phys. Lett. **112**, 161601 (2018).
[17] Gerardo J. Escalera Santos, M. Rivera, and P. Parmananda, Phys. Rev. Lett. **92**, 230601 (2004).
[18] M. Nurujjaman, A. N. Sekar Iyengar, and P. Parmananda, Phys. Rev. E **78**, 026406 (2008).
[19] J. J. Collins, C. C. Chow, and T. T. Imhoff, Phys. Rev. E **52**, R3321(R) (1995).
[20] M. Rivera, Gerardo J. Escalera Santos, J. Uruchurtu-Chavarin, and P. Parmananda, Phys. Rev. E **72**, 030102(R) (2005).
[21] J. Escorcia-Garcia, V. Agarwal, and P. Parmananda, Appl. Phys. Lett. **94**, 133103 (2009).
[22] T. Roy, S. Rumandla, V. Agarwal, and P. Parmananda, J. Appl. Phys. **122**, 124904 (2017).
[23] L. Gammaitoni, P. Hänggi, P. Jung, and F. Marchesoni, Rev. Mod. Phys. **70**, 223 (1998).
[24] V. S. Anishchenko, M. Safonova, and L. O. Chua, J. Circ., Syst. Comput. **3**, 553 (1993).
[25] D. T. W. Chik, Y. Wang, and Z. D. Wang, Phys. Rev. E **64**, 021913 (2001).
[26] K. Joshi, I. Tiwari, A. Nandi, and P. Parmananda, Phys. Rev. E **98**, 012218 (2018).
[27] B. Xu, J. Li, and J. Zheng, J. Phys. A: Math. Gen. **36**, 11969 (2003).
[28] B. Xu, F. Duan, and F. Chapeau-Blondeau, Phys. Rev. E **69**, 061110 (2004).
[29] S. Jiang, F. Guo, Y. Zhou, and T. Gu, Phys. A (Amsterdam, Neth.) **375**, 483 (2007).
[30] A. Karantonis and S. Nakabayashi, Chem. Phys. Lett. **347**, 133 (2001).
[31] Gerardo J. Escalera Santos, M. Rivera, M. Eiswirth, and P. Parmananda, Phys. Rev. E **70**, 021103 (2004).